



## Original article

# Lobar pulmonary perfusion quantification with dual-energy CT angiography: Interlobar variability and relationship with regional clot burden in pulmonary embolism

Hye Ju Lee<sup>a,\*</sup>, Mark Wanderley<sup>a</sup>, Vivian Cardinal da Silva Rubin<sup>a</sup>, Ana Clara Tude Rodrigues<sup>b</sup>, Amanda Rocha Diniz<sup>b</sup>, Jose Rodrigues Parga<sup>a</sup>, Marcelo Britto Passos Amato<sup>c</sup>

<sup>a</sup> Department of Radiology, Hospital das Clinicas, Faculdade de Medicina, Universidade de Sao Paulo, Sao Paulo, SP, Brazil

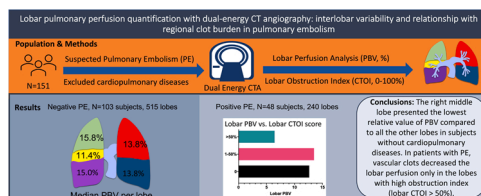
<sup>b</sup> Echocardiography Laboratory, Department of Radiology, Hospital das Clinicas, Faculdade de Medicina, Universidade de Sao Paulo, Sao Paulo, SP, Brazil

<sup>c</sup> Pneumology Division, Instituto do Coracao, Hospital das Clinicas, Faculdade de Medicina, Universidade de Sao Paulo, Sao Paulo, SP, Brazil

## HIGHLIGHTS

- Semi-automated tools enable assessment of lobar perfusion with Dual-Energy CTA.
- The pulmonary perfusion is heterogeneously distributed along the pulmonary lobes.
- Lobar perfusion was decreased only in the lobes with high vascular obstruction index.

## GRAPHICAL ABSTRACT



## ARTICLE INFO

## Keywords:

Pulmonary embolism  
Computed tomography angiography  
Pulmonary perfusion  
Blood volume  
Dual-energy computed tomography (DECT)

## ABSTRACT

**Purpose:** Semi-automated lobar segmentation tools enable an anatomical assessment of regional pulmonary perfusion with Dual-Energy CTA (DE-CTA). We aimed to quantify lobar pulmonary perfusion with DE-CTA, analyze the perfusion distribution among the pulmonary lobes in subjects without cardiopulmonary diseases and assess the correlation between lobar perfusion and regional endoluminal clots in patients with acute pulmonary embolism (PE).

**Methods:** We evaluated 151 consecutive subjects with suspected PE and without cardiopulmonary comorbidities. DE-CTA derived perfused blood volume (PBV) of each pulmonary lobe was measured applying a semi-automated lobar segmentation technique. In patients with PE, blood clot location was assessed, and CT-based vascular obstruction index of each lobe (CTOI<sub>lobe</sub>) was calculated and classified into three groups: CTOI<sub>lobe</sub> = 0, low CTOI<sub>lobe</sub> (1–50%) and high CTOI<sub>lobe</sub> (>50%).

**Results:** Among patients without PE (103/151, 68.2%), median lobar PBV was 13.7% (IQR 10.2–18.0%); the right middle lobe presented lower PBV when compared to all the other lobes ( $p < .001$ ). In patients with PE (48/151, 31.8%), lobar PBV was 12.6% (IQR 9.6–15.7%), 13.7% (IQR 10.1–16.7%) and 6.5% (IQR 5.1–10.2%) in the lobes with CTOI<sub>lobe</sub> = 0, low CTOI<sub>lobe</sub> and high CTOI<sub>lobe</sub> scores, respectively, with a significantly decreased PBV in the lobes with high CTOI<sub>lobe</sub> score ( $p < .001$ ). ROC analysis of lobar PBV for prediction of high CTOI<sub>lobe</sub> score revealed AUC of 0.847 (95%CI 0.785–0.908).

**Abbreviations:** CTOI, Computed tomography obstruction index; DE-CTA, Dual-energy computed tomography angiography; PBV, Perfused blood volume.

\* Correspondence to: Department of Radiology, Hospital das Clinicas, University of Sao Paulo, R. Dr Ovidio Pires de Campos, 75, Sao Paulo, SP 05403-010, Brazil.

E-mail address: [hvejulee@gmail.com](mailto:hvejulee@gmail.com) (H.J. Lee).

<https://doi.org/10.1016/j.ejro.2022.100428>

Received 22 April 2022; Received in revised form 18 May 2022; Accepted 28 May 2022

2352-0477/© 2022 The Authors. Published by Elsevier Ltd. This is an open access article under the CC BY-NC-ND license (<http://creativecommons.org/licenses/by-nc-nd/4.0/>).

**Conclusion:** Pulmonary perfusion was heterogeneously distributed along the pulmonary lobes in patients without cardiopulmonary diseases. In patients with PE, the lobes with high vascular obstruction score ( $CTOI_{lobe} > 50\%$ ) presented a decreased lobar perfusion.

## 1. Introduction

Dual Energy computed tomography is a single acquisition technique that permits the decomposition of different materials within an anatomic region, based on the differences in the attenuation of its elements (e.g., water, iodine, and calcium) at different energy levels [1,2]. The application of Dual Energy technique in Pulmonary CT Angiography (DE-CTA) permits the generation of iodine distribution maps and is considered a surrogate of dynamic studies of pulmonary perfusion [3]. Previous studies demonstrated a reduced global pulmonary perfusion estimated by DE-CTA (i.e., a reduction in the mean iodine distribution in the entire lung) in patients with acute pulmonary embolism (PE), and also a correlation between global perfusion and adverse clinical outcomes in patients with PE [4–7].

Pulmonary perfusion distribution is influenced by several factors beyond vascular obstruction, including gravity, pulmonary density, and structural features of the lung [8]. Regional gradients of pulmonary perfusion were previously demonstrated in studies using electron-beam CT (EBCT), scintigraphy, single-photon emission computed tomography (SPECT), magnetic resonance imaging (MRI), and DE-CTA [9–13]. These quantitative studies of regional pulmonary perfusion were based on non-anatomical zonal division models of the lungs (e.g., upper-intermediate-lower zones, or ventral-intermediate-dorsal zones). Pulmonary lobes, however, are separated by fissures, features a particular structural anatomy, and are supplied by an independent vascular tree originated from the main pulmonary arteries. Impairments in the blood flow on a specific arterial branch, for example, might affect the regional perfusion of the lobe that is supplied by its distal branches, with minor or non-repercussion in the nearby parenchyma of a neighboring lobe, even when located within the same zone. One single recent study compared lobar and zonal quantitative perfusion parameters using DE-CTA and reported a higher accuracy of the lobar perfusion analysis in the prediction of PE [14].

The application of semi-automated lung lobe segmentation techniques can enable the perfusion quantification of each pulmonary lobe and permits a more anatomical approach of regional blood flow distribution. Thus, the first aim of this study was to assess the lobar distribution of pulmonary perfusion with DE-CTA in subjects without cardiopulmonary diseases. Second, we investigated the correlation

between regional endoluminal clots and lobar perfusion in patients with PE.

## 2. Materials and methods

### 2.1. Study design and population

The study retrospectively evaluated in-hospital patients of our tertiary referral center that underwent DE-CTA for suspected PE between April 2016 and July 2019. Clinical database originated from a previous study in which patients had already signed an informed consent form and was approved by local Institutional Review Board.

Among 233 eligible subjects with suspected PE, patients with underlying cardiopulmonary diseases, CT scans with poor contrast enhancement (attenuation  $< 200$  Hounsfield Units (HU) in the pulmonary trunk) and those exams with technical limitations that precluded images post-processing were excluded. A total of 151 patients were included in the study.

### 2.2. DE-CTA image acquisition protocol

DE-CTA examinations were performed on a single-tube DE-CT scanner (Discovery CT750 HD; GE Healthcare, Chicago, Ill) with rapid kilovoltage peak switching (140 and 80 kVp), tube current of 630 mA, pitch of 1.375, rotation time of 0.5 s and collimation of  $64 \times 0.625$  mm. Intravenous iodinated contrast material (1.0 ml/kg of iobitridol - Xenetix 300; Guerbet, Villepinte, France) was infused at 4.0 ml/sec, followed by a 50 ml saline flush at 5.0 ml/sec. A region of interest (ROI) was placed over the pulmonary artery at the level of the carina and acquisition in caudo-cranial direction started seven seconds after attenuation in the ROI achieved 100 HU.

### 2.3. Evaluation of DE-CTA findings

#### 2.3.1. Quantitative analysis of DE-CTA

An automated algorithm (GSI viewer tool; AW Workstation; GE Healthcare) generated the iodine pulmonary maps (Fig. 1). One thoracic radiologist performed the pulmonary lobes segmentation using Chest Imaging Platform (CIP, Applied Chest Imaging Laboratory; Boston,

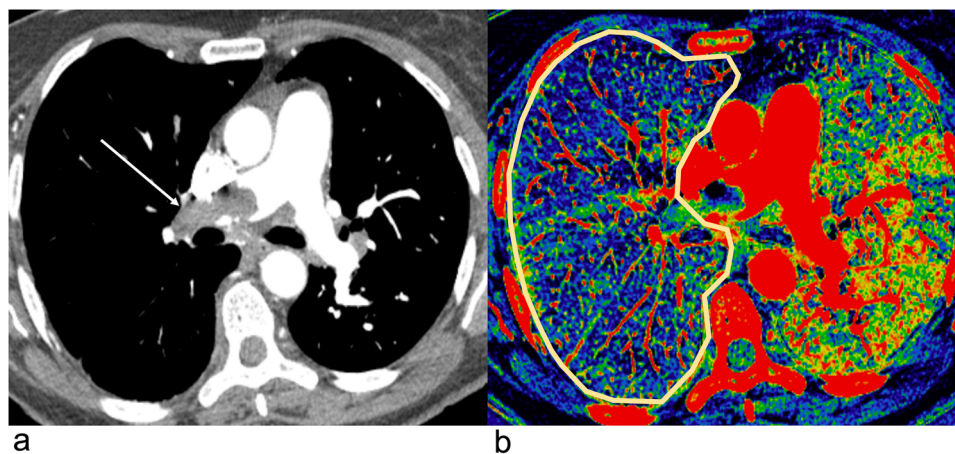


**Fig. 1.** 52-year-old woman with acute pulmonary embolism. CTA axial image shows a filling defect in the right pulmonary artery (arrow in a). A diffusely reduced iodine density in the right lung (area demarcated by yellow line and represented by blue color) is visualized in the color-coded pulmonary iodine map (b). (For interpretation of the references to colour in this figure legend, the reader is referred to the web version of this article.)

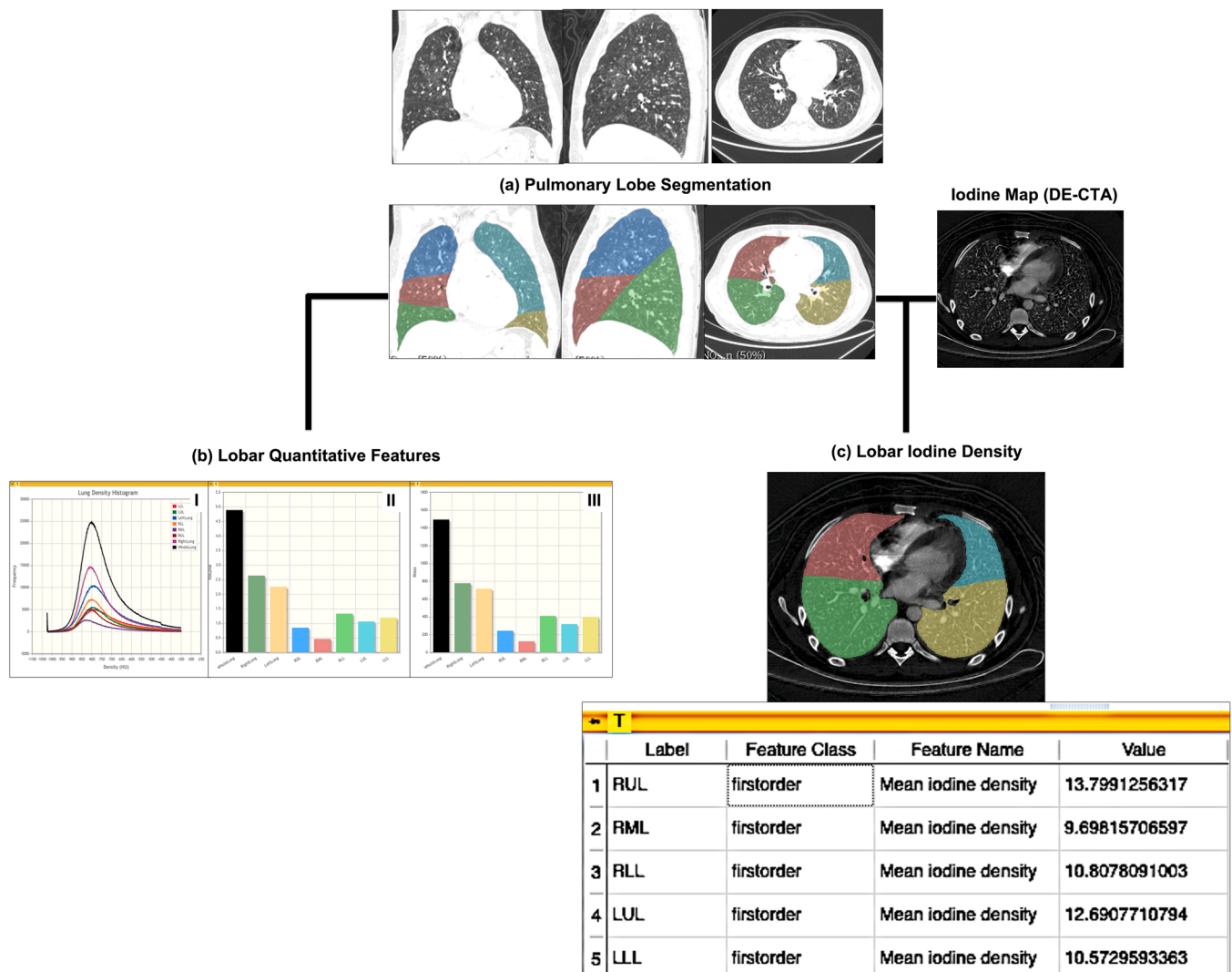


**Fig. 2.** Schematic representation of image postprocessing steps. Following CT acquisition, pulmonary lobes were segmented using Interactive Lobe Segmentation tool from 3D Slicer platform (<http://www.slicer.org>). A small number of fiducial points (5–10) was manually selected along the right and left oblique fissures and the right horizontal fissure. A label map delimiting each lung lobe was created by the platform, based on the user-specified fiducial points (a). In b, quantitative features of the whole lung and of each lung lobe were obtained (I - lung density histogram, II - lung volume, III - lung mass). Iodine density of each lung lobe (c) was acquired after merging segmented lung label map with iodine map (represented in grayscale). RUL, right upper lobe; RML, right middle lobe; RLL, right lower lobe; LUL, left upper lobe; LLL, left lower lobe.

Massachusetts, USA) extension [15,16] for open-source software platform 3D Slicer software, version 4.8.2 [17] (<http://www.slicer.org>). The Interactive Lobe Segmentation tool permitted a semi-automated segmentation of the lung lobes by selecting a small number of fiducial points (5–10) on each fissure.

The Parenchyma Analysis module within CIP provided the volume, mass, and density of the whole lung and of each lung lobe. Radiomics extension module within 3D Slicer allowed acquisition of mean iodine density of the whole lung and of each lung lobe, by merging iodine map and segmented lung images (Fig. 2).

A relative value of pulmonary perfused blood volume (PBV) was calculated by normalizing the iodine density (mg/ml) of each lung lobe by the iodine density of the pulmonary artery (region of interest set in the pulmonary trunk), according to the equation.

$$PBV(\%) = \frac{\text{mean iodine density of lung lobe}}{\text{iodine density of pulmonary artery}} \times 100$$

### 2.3.2. Blood clot distribution and lobar vascular obstruction index

Location and distribution of blood clots of all exams with positive PE

were assessed and recorded. To determinate the CT-based vascular obstruction index of each pulmonary lobe (CTOI<sub>lobe</sub>), a semiquantitative method adapted from Qanadli et al. [18], was performed by one thoracic radiologist that was blinded to the iodine maps. The arterial tree of the lung was divided according to the number of segmental arteries of each pulmonary lobe (i.e., three in the right upper lobe, five in the left upper lobe – including lingula, two in the right middle lobe, and five in each lower lobe, totalizing 20 segmental arteries). Clot burden was calculated using the formula  $CTOI_{lobe} = \{ \frac{\sum(n \times d)}{t} \times 100 \}$ , where *n* is the number of segmental vessels arising distally, *d* is the degree of obstruction (0, patent vessel; 1, partial occlusion; 2, completely occluded vessel) and *t* is the maximum achievable score for each lobe (six for the right upper lobe, ten for the left upper lobe, four for the right middle lobe and ten for each lower lobe). Central clots scored in all the distally located lobes and a subsegmental embolus was considered a partial occlusion in the corresponding segmental artery [19].

Pulmonary lobes were classified into three groups based on CTOI<sub>lobe</sub> score: (1) without obstruction (score = 0), (2) low CTOI<sub>lobe</sub> score (1–50%) and (3) high CTOI<sub>lobe</sub> score (>50%).

Regarding distribution, blood clots were considered peripheral when

**Table 1**  
Clots location in patients with PE.

	Positive PE (N = 48)
Number of lobes with clots per patient	
1	12 (25.0)
2	9 (18.8)
3	7 (14.6)
4	5 (10.4)
5	15 (31.3)
Clot location	
RUL	27 (56.3)
RML	21 (43.8)
RLL	41 (85.4)
LUL	26 (54.2)
LLL	31(64.6)
Whole lung CTOI	
1–50%	41 (85.4)
51–100%	7 (14.6)

Note – Data corresponds to the number and percentage of patients. RUL, right upper lobe; RML, right middle lobe; RLL, right lower lobe; LUL, left upper lobe; LLL, left lower lobe

located in segmental or subsegmental arteries and central when located in any artery located centrally to segmental arteries, including the pulmonary trunk, main pulmonary arteries, and interlobar/lobar arteries.

**2.4. Statistical analysis**

Continuous variables are expressed as medians and interquartile range (IQR) and categorical variables as numbers (n) and percentages (%). Mann-Whitney U test was used to compare continuous variables. Chi-square test and Fisher’s exact test were used to compare categorical variables. The Spearman correlation coefficient (*r*) was used for correlation analyses between lung density and lobar PBV. Value of *r* from 0 to 0.30, from 0.30 to 0.50, from 0.50 to 0.70, from 0.70 to 0.90. and greater than 0.90 were considered negligible, low, moderate, high, and very high correlations, respectively [20].

The association of clot distribution (central vs. peripheral), clot location (i.e., in which lobe the clot is located), and CTOI<sub>lobe</sub> score with the lobar PBV was assessed using linear regression analysis. In order to test the independent association between each variable and lobar PBV, a multivariate linear regression model was applied. The ability of lobar PBV in the prediction of high CTOI<sub>lobe</sub> score was investigated using the

receiver operating characteristic curve (ROC) and analyzing the area under the curve (AUC).

*P* < .05 was considered significant. All data was analyzed using SPSS (IBM SPSS Statistics for Windows, Version 20.0. Armonk, NY: IBM Corp). Graphs were performed using GraphPad Prism version 8.1.1 for macOS, GraphPad Software.

**3. Results**

Forty-eight out of 151 patients presented PE (31.8%). Median age was 50 years (IQR 33.5–64.0), with no significant differences between the groups of patients with and without PE (56 [IQR 32.5–67.5] vs. 48 [IQR 34.5–62.5], *p* = .227). There was a female predominance in both groups (35/48 [72.9%] with PE and 72/103 [69.9%] without PE), with no significant differences between the groups (*p* = .848).

Most patients with positive PE (36/48, 75%) presented clots in two or more lobes and the right lower lobe was the most affected (41/48, 85.4%) (Table 1).

Lobar perfusion analysis and other regional quantitative features are summarized in Table 2. In patients without vascular obstructions (negative PE), there was a significant difference in the lung density between the lobes (*p* < .001), with decreased lung density in the right middle lobe when compared to the right upper lobe (*p* = .007) and to both lower lobes (*p* < .001). Still among patients without PE, there was a reduced PBV in the right middle lobe when compared to both upper and lower lobes (*p* < .001). A non-significant difference of the PBV between the remaining lobes was observed, with slightly higher PBV in the upper and lower lobes of the right lung compared to the lobes of the left lung (*p* = .185) (Fig. 3). The Spearman’s correlation coefficient between lung PBV and lung density in the exams without PE was 0.57 (*p* < .001).

Among the 240 pulmonary lobes from the 48 patients with positive PE, 146 lobes (60.8%) presented blood clots. CTOI<sub>lobe</sub> scored between 1% and 50% (low CTOI<sub>lobe</sub>) in most of the lobes with blood clots (72.6%, 106/146) and above 50% (high CTOI<sub>lobe</sub>) in 27.4% of the lobes (40/146). Nearly two thirds of the lobes presented only peripheral clots (64.4%, 94/146) and the remaining lobes presented both peripheral and central clots (32.2%, 47/146) or only central clots (3.4%, 5/146).

Clots distribution according to the lobar CTOI<sub>lobe</sub> score are shown in Fig. 4. Most of the lobes with low CTOI<sub>lobe</sub> score exhibited clots only in peripheral arteries (84/106, 79.2%). Central clots were detected in three quarters of the lobes with high CTOI<sub>lobe</sub> score (30/40), with predominance of the combination of both central and peripheral clots (26/40,

**Table 2**  
Regional quantitative features and lobar perfusion in patients with and without PE.

	RUL	RML	RLL	LUL	LLL	Total Lung
<b>Lung volume, ml</b>						
Negative PE	649 (522–887)	355 (285–452)	788 (543–1047)	789 (669–1089)	657 (437–912)	3147 (2590–4301)
Positive PE	669 (512–858)	323 (281–422)	730 (502–933)	842 (710–982)	639 (469–826)	3285 (2714–3753)
<b>Lung mass, g</b>						
Negative PE	186 (161–218)	91 (70–107)	231 (189–284)	225 (191–263)	201 (160–250)	939 (800–1094)
Positive PE	184 (156–201)	83 (69–93)	216 (181–247)	215 (187–242)	186 (165–211)	864 (779–1000)
<b>Lung density, g/ml</b>						
Negative PE	0.28 (.23–0.32)	0.24 (.20–0.28)	0.30 (.25–0.38)	0.26 (.22–0.32)	0.32 (.26–0.38)	0.28 (.24–0.34)
Positive PE	0.26 (.23–0.30)	0.24 (.21–0.27)	0.29 (.25–0.39)	0.26 (.23–0.32)	0.31 (.25–0.37)	0.27 (.24–0.34)
<b>PBV, %</b>						
Negative PE	15.8 (11.5–20.3)	11.4 (8.7–14.4)	15.0 (10.6–17.7)	13.8 (10.4–18.0)	13.8 (10.4–18.7)	14.6 (10.5–18.1)
Positive PE	14.3 (10.6–17.6)	9.7 (8.0–11.9)	13.1 (9.0–15.8)	13.3 (9.6–16.5)	13.0 (9.8–15.5)	13.0 (9.5–15.3)

Note – Data correspond to median with interquartile range in parentheses. RUL, right upper lobe; RML, right middle lobe; RLL, right lower lobe; LUL, left upper lobe; LLL, left lower lobe

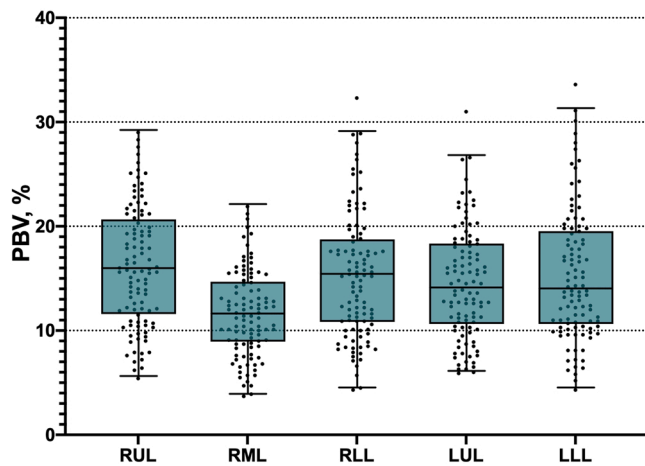


Fig. 3. Box and whisker plot with individual data points illustrating the variation of PBV in the lobes of patients with negative PE. Right middle lobe presented a significantly reduced PBV ( $p < .001$ ). RUL, right upper lobe; RML, right middle lobe; RLL, right lower lobe; LUL, left upper lobe; LLL, left lower lobe.

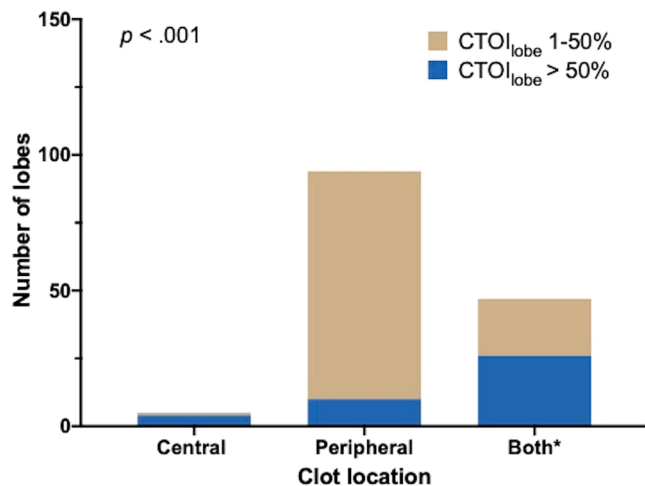


Fig. 4. Graph chart illustrating blood clot distribution according to lobar CTOLobe score. \* central and peripheral clots within the same lobe.

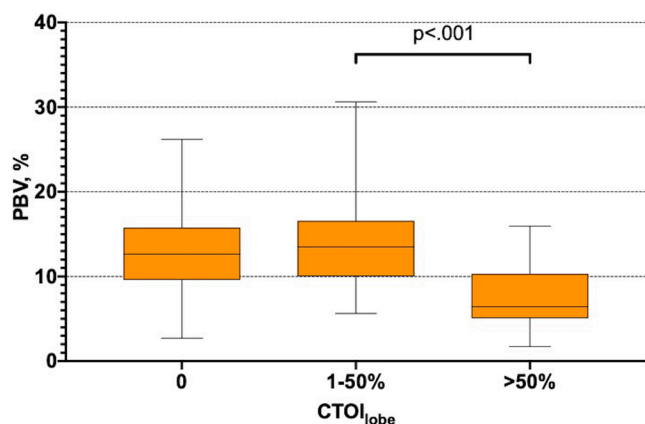


Fig. 5. Box and whisker plot illustrating the PBV in the lobes without vascular obstruction (score = 0), with low CTOLobe score (1–50%) and high CTOLobe score (>50%) in the patients with PE.

65%).

The median lobar PBV in the lobes of patients without PE was 13.7% (IQR 10.2–18.0). In patients with PE, lobar PBV in the lobes with CTOLobe score = 0, low CTOLobe score and high CTOLobe score were, respectively, 12.6 (IQR 9.6–15.7), 13.7 (IQR 10.1–16.7) and 6.5 (IQR 5.1–10.2). PBV was significantly decreased in the lobes with high CTOLobe score compared to all the other groups ( $p < .001$ ), with no significant differences in the lobar PBV between the remaining groups ( $p = .957$ ) (Fig. 5).

Linear regression analysis of the influence of clot distribution, clot location, and CTOLobe score on lobar PBV is demonstrated in Table 3. In univariate analysis, central clots and high CTOLobe score negatively influenced lobar PBV ( $p = .001$  and  $p < .001$ , respectively), and there was a negative but not significant influence of the location in the right middle lobe on PBV ( $p = .07$ ). In multivariate analysis, only high CTOLobe score independently influenced lobar PBV ( $p < .001$ ). ROC analysis of lobar PBV for prediction of high CTOLobe score revealed AUC of 0.847 (Fig. 6).

#### 4. Discussion

Lobar distribution of pulmonary perfusion could be quantitatively assessed with DE-CTA in a few and semi-automated steps in the present study. We observed that pulmonary perfusion is not homogeneously distributed between the lobes in patients without vascular obstructions and that, in patients with PE, a high regional clot load score is associated with a decrease in the lobar PBV.

##### 4.1. Interlobar PBV distribution

In patients without cardiopulmonary diseases and negative PE, a predictable heterogeneous perfusion distribution was observed among the pulmonary lobes, with a significantly reduced PBV in the right middle lobe compared to all the other lobes ( $p < .001$ ).

Earlier studies of pulmonary perfusion using EBCT, nuclear imaging and MRI showed a decreasing perfusion from dorsal to ventral regions in the supine position in healthy humans, with a more uniform distribution in the prone position [9–12]. Felloni et al. [13] also demonstrated a significant gradient between the posterior (i.e., dependent) and anterior (i.e., non-dependent) lung zones using DE-CTA in a group of patients without cardiopulmonary diseases. The dorsal-to-ventral gradient might be one possible explanation for the significantly lower PBV in the right middle lobe observed in the present study, as most of the volume of this lobe is situated in the ventral lung zone (i.e., in the non-dependent zone in the supine position), whereas upper and lower lobes are distributed along both dependent and non-dependent zones.

The gravitational gradient of pulmonary perfusion was widely demonstrated by earlier studies since 1960 s [21–25], but later studies including computational and experimental models, as well as imaging methods with improved spatial resolution demonstrated that pulmonary perfusion distribution is beyond the linear zonal gravitational model proposed by West et al. [26]. Moreover, one more factor that should be considered in the vertical gradient of the pulmonary perfusion distribution is the influence of the lung density. Dependent regions of the lung usually present higher density (mass/volume) than non-dependent regions, due to the lung compression. Consequently, the quantification of regional perfusion, when measured per unit of pulmonary volume, might be significantly increased in the higher density (i.e., dependent) regions, without necessarily meaning a physiological increase in the pulmonary blood flow. Hopkins et al. [27] observed that both pulmonary perfusion (measured per unit volume, ml/min/cm<sup>3</sup>) and lung density (g/ml) were significantly higher in the dependent regions of the lung in a group of healthy patients using MRI. When perfusion was normalized by lung density (i.e., expressed in ml/min/g), there was a significant reduction in the vertical gradient of pulmonary perfusion. In concordance with the findings of Hopkins et al., we could demonstrate a

**Table 3**  
Influence of clot distribution and location, and CTOI<sub>lobe</sub> score on lobar PBV values.

	Regression coefficient B	Standardized regression coefficient $\beta$	P-value	Regression coefficient B	Standardized regression coefficient $\beta$	P-value
	Univariate analysis			Multivariate analysis		
CTOI <sub>lobe</sub> > 50% (ref 1–50%)	-6.689	-.503	< .001	-6.236	-.469	< .001
Central clot <sup>1</sup> (ref peripheral <sup>2</sup> )	-3.388	-.274	.001	-0.400	-.032	.70
RUL (ref RLL)	1.147	.075	.43	1.475	.097	.25
RML (ref RLL)	-2.934	-.174	.07	-1.164	-.069	.42
LUL (ref RLL)	0.34	.002	.98	0.168	.011	.90
LLL (ref RLL)	1.097	.076	.43	0.364	.025	.77
Constant				14.116		< .001

Note <sup>1</sup> includes the lobes with only central clots or with both central and peripheral clots. <sup>2</sup> includes the lobes with only peripheral clots. Ref, reference.

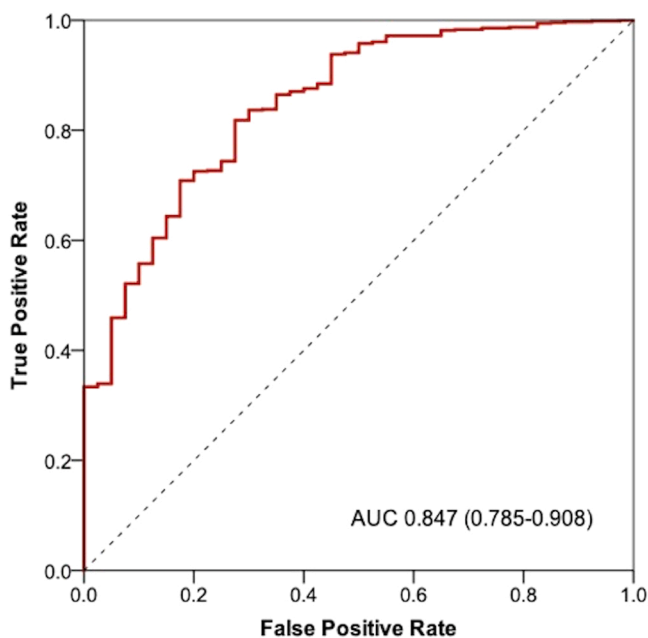


**Fig. 6.** Receiver operating characteristic (ROC) curve of lobar PBV for prediction of high vascular obstruction score (CTOI<sub>lobe</sub>>50%).

moderate correlation between lobar PBV and lobar density ( $r = 0.57$ ,  $p < .001$ ).

The distribution of blood flow within the lungs, however, is not exclusively influenced by vertical gradient [28–30]. The presence of perfusion heterogeneity within isogravitational planes of the lung demonstrated by previous studies suggests that the anatomic structure might significantly influence the blood flow and that the geometry of the pulmonary vascular tree is determinant in the perfusion distribution [31–33].

In an experimental study using SPECT, Hakim et al. [34] reported a marked central-to-peripheral gradient in the perfusion distribution, possibly related to the influence of the length and the branching of the conducting vessels in the vascular resistance and, consequently, in the blood flow. Each lung lobe presents an independent branching structure, comprising equivalent proportions of generations of vascular branches. As a result, central-to-peripheral gradient might have minor influence in the lobar distribution of pulmonary perfusion. Indeed, in our study, the upper and lower lobes, which are also less influenced by the vertical gradient, did not present significant differences in the PBV.

#### 4.2. Correlation between lobar PBV and lobar CTOI

As expected, lobar PBV correlated negatively to CTOI<sub>lobe</sub> score, with

AUC of 0.847 ( $p < .001$ ) in predicting high lobar clot load score (CTOI<sub>lobe</sub> > 50%). This result is in concordance with global PBV analysis performed by Meinel et al. [6], that showed a significant negative correlation between global PBV and Qanadli obstruction score ( $r = -0.46$ ;  $p < .001$ ) of the whole lung, in a similar group of patients with PE and without other thoracic comorbidities.

A clot load score of less than or equal to 50%, however, did not decrease the lobar PBV when compared to lobes without vascular obstruction in our study. In a normal lung, high-blood-flow regions are usually matched with high-ventilation regions and vice versa. In PE, pulmonary clots are preferentially distributed to high-blood-flow regions, redistributing blood to previously low-blood-flow regions, with no change in regional ventilation, resulting in ventilation/perfusion mismatch and producing hypoxemia [35]. The redistribution of blood flow, without significant reduction in the perfused volume, might be a possible explanation for the results of our study. When clots were located only in peripheral branches, as occurred in most of the lobes with low CTOI<sub>lobe</sub> score (84/106, 79.2%), the blood flow might have been redirected to non-obstructed low-blood-flow branches within the same lobe, maintaining the total lobar PBV. On the other hand, in the presence of central clots, that were mostly found in the lobes with high CTOI<sub>lobe</sub> score (30/40, 75%), blood flow might have been redirected to the neighboring lobes without vascular obstruction, consequently reducing lobar PBV.

A wide spectrum of diseases may result in diminished regional pulmonary perfusion. Acute PE is one of the most common causes, but chronic thromboembolic pulmonary hypertension (CTEPH), extrinsic vascular compressions (e.g., hilar masses, mediastinitis or previous local radiation therapy), regional parenchymal diseases (e.g., bullous emphysema or post-inflammatory sequelae) and congenital anomalies of pulmonary arterial branches are some potential clinical applications of lobar perfusion analysis with DE-CTA. As practical examples, quantitative assessment of lobar perfusion could be useful in patients with CTEPH before and after embolectomy, in pulmonary artery reconstructions of congenital anomalies and preoperative planning of lung volume reduction surgeries in severe chronic obstructive pulmonary disease (COPD) [36–38].

#### 4.3. Limitations

This is a retrospective study performed in a single institution. To minimize the influence in PBV, a significant proportion of the patients were excluded due to the coexistence of underlying cardiopulmonary diseases, such as emphysema, fibrosing interstitial lung disease, pneumonia, and pulmonary malignancies. Consequently, our results might not be applicable in a larger population of patients with thoracic comorbidities.

The study comprises a heterogeneous group of patients that were hospitalized in our institution due to a variety of causes, including oncologic and infectious diseases, postoperative care, and trauma. Despite the exclusion of cardiopulmonary diseases, patients were not

stratified by the remaining comorbidities, even though they were not expected to directly influence the lobar PBV.

Finally, we did not perform a correlative analysis of lobar PBV with prognostic parameters, such as laboratorial biomarkers, signs of right ventricular dysfunction or patients clinical outcome; therefore, the prognostic value of our findings might be a possible direction for future investigation.

## 5. Conclusions

Lobar quantification of PBV with DE-CTA is a feasible approach that might be clinically applicable in several vascular and non-vascular causes of diminished regional pulmonary perfusion. Interlobar distribution of PBV was demonstrated in our study in subjects without cardiopulmonary diseases. In patients with PE and without other thoracic comorbidities, the lobar PBV negatively correlated to the clot load when obstruction score was above 50%, whereas a low blood clot load score did not significantly reduce PBV.

## Funding

This work was supported by Financiadora de Estudos e Projetos - FINEP (01140089000).

## CRedit authorship contribution statement

**Hye Ju Lee:** Conceptualization, Formal analysis, Investigation, Writing – original draft. **Mark Wanderley:** Investigation. **Vivian Cardinal da Silva Rubin:** Formal analysis, Investigation. **Ana Clara Tude Rodrigues:** Methodology, Investigation. **Amanda Rocha Diniz:** Investigation. **Jose Rodrigues Parga:** Validation, Writing – review & editing, Supervision. **Marcelo Brito Passos Amato:** Conceptualization, Supervision, Project administration, Funding acquisition.

## Ethical statement

Clinical database originated from a previous study in which patients had already signed an informed consent form. We obtained institutional review board (IRB) approval of the Ethical Committee at Hospital das Clinicas, University of Sao Paulo.

## Declaration of Competing Interest

The authors report no declarations of interest.

## References

- [1] R.E. Alvarez, A. Macovski, Energy-selective reconstructions in X-ray computerized tomography, *Phys. Med. Biol.* 21 (5) (1976) 733–744, <https://doi.org/10.1088/0031-9155/21/5/002>.
- [2] X. Liu, L. Yu, A.N. Primak, C.H. McCollough, Quantitative imaging of element composition and mass fraction using dual-energy CT: three-material decomposition, *Med. Phys.* 36 (5) (2009) 1602–1609, <https://doi.org/10.1118/1.3097632>.
- [3] M.K. Fuld, A.F. Halaweish, S.E. Haynes, A.A. Divekar, J. Guo, E.A. Hoffman, Pulmonary perfused blood volume with dual-energy CT as surrogate for pulmonary perfusion assessed with dynamic multidetector CT, *Radiology* 267 (3) (2013) 747–756, <https://doi.org/10.1148/radiol.12112789>.
- [4] R.W. Bauer, C. Frellesen, M. Renker, B. Schell, T. Lehnert, H. Ackermann, U. J. Schoepf, V. Jacobi, T.J. Vogl, J.M. Kerl, Dual energy CT pulmonary blood volume assessment in acute pulmonary embolism - correlation with D-dimer level, right heart strain and clinical outcome, *Eur. Radiol.* 21 (9) (2011) 1914–1921, <https://doi.org/10.1007/s00330-011-2135-1>.
- [5] A. Sakamoto, I. Sakamoto, H. Nagayama, H. Koike, E. Sueyoshi, M. Uetani, Quantification of lung perfusion blood volume with dual-energy CT: assessment of the severity of acute pulmonary thromboembolism, *Ajr. Am. J. Roentgenol.* 203 (2) (2014) 287–291, <https://doi.org/10.2214/AJR.13.11586>.
- [6] F.G. Meinel, A. Graef, F. Bamberg, S.F. Thieme, F. Schwarz, W.H. Sommer, C. Neurohr, C. Kupatt, M.F. Reiser, T.R. Johnson, Effectiveness of automated quantification of pulmonary perfused blood volume using dual-energy CTPA for the severity assessment of acute pulmonary embolism, *Invest. Radiol.* 48 (8) (2013) 563–569, <https://doi.org/10.1097/RLI.0b013e3182879482>.
- [7] E. Sueyoshi, S. Tsutsui, T. Hayashida, K. Ashizawa, I. Sakamoto, M. Uetani, Quantification of lung perfusion blood volume (lung PBV) by dual-energy CT in patients with and without pulmonary embolism: preliminary results, *Eur. J. Radiol.* 80 (3) (2011) e505–e509, <https://doi.org/10.1016/j.ejrad.2010.10.011>.
- [8] S.R. Hopkins, M.O. Wielpütz, H.U. Kauczor, Imaging lung perfusion, *J. Appl. Physiol.* (Bethesda, Md.: 1985) 113 (2) (2012) 328–339, <https://doi.org/10.1152/japplphysiol.00320.2012>.
- [9] A.T. Jones, D.M. Hansell, T.W. Evans, Pulmonary perfusion in supine and prone positions: an electron-beam computed tomography study, *J. Appl. Physiol.* (Bethesda, Md.: 1985) 90 (4) (2001) 1342–1348, <https://doi.org/10.1152/jappl.2001.90.4.1342>.
- [10] S. Nyérén, M. Mure, H. Jacobsson, S.A. Larsson, S.G. Lindahl, Pulmonary perfusion is more uniform in the prone than in the supine position: scintigraphy in healthy humans, *J. Appl. Physiol.* (Bethesda, Md.: 1985) 86 (4) (1999) 1135–1141, <https://doi.org/10.1152/jappl.1999.86.4.1135>.
- [11] H.M. Almqvist, J. Palmer, B. Jonson, P. Wollmer, Pulmonary perfusion and density gradients in healthy volunteers, *J. Nucl. Med.: Off. Publ., Soc. Nucl. Med.* 38 (6) (1997) 962–966.
- [12] H. Suzuki, Y. Sato, M. Shindo, H. Yoshioka, T. Mizutani, M. Onizuka, Y. Sakakibara, Prone positioning improves distribution of pulmonary perfusion: noninvasive magnetic resonance imaging study in healthy humans, *Eur. Radiol.* 18 (3) (2008) 522–528, <https://doi.org/10.1007/s00330-007-0808-6>.
- [13] P. Felloni, A. Duhamel, J.B. Faivre, J. Giordano, S. Khung, V. Deken, J. Remy, M. Remy-Jardin, Regional distribution of pulmonary blood volume with dual-energy computed tomography: results in 42 subjects, *Acad. Radiol.* 24 (11) (2017) 1412–1421, <https://doi.org/10.1016/j.acra.2017.05.003>.
- [14] R. Singh, R.Z. Nie, F. Homayounieh, B. Schmidt, T. Flohr, M.K. Kalra, Quantitative lobar pulmonary perfusion assessment on dual-energy CT pulmonary angiography: applications in pulmonary embolism, *Eur. Radiol.* 30 (5) (2020) 2535–2542, <https://doi.org/10.1007/s00330-019-06607-9>.
- [15] R. San José Estépar, J.C. Ross, R. Harmouche, et al., Chest imaging platform: an open-source library and workstation for quantitative chest imaging, *Am. Thorac. Soc. Int. Conf. Abstr.* (2015). (<https://www.atsjournals.org/doi/abs/10.1164/ajrccm-conference.2015.191.1.MeetingAbstracts.A4975>).
- [16] J. Onieva, J. Ross, R. Harmouche, et al., Chest imaging platform: an open-source library and workstation for quantitative chest imaging, *Int. J. Comput. Assist. Radio. Surg. Suppl. 1* (11) (2016) S40–S41.
- [17] A. Fedorov, R. Beichel, J. Kalpathy-Cramer, J. Finet, J.C. Fillion-Robin, S. Pujol, C. Bauer, D. Jennings, F. Fennessy, M. Sonka, J. Buatti, S. Aylward, J.V. Miller, S. Pieper, R. Kikinis, 3D slicer as an image computing platform for the quantitative imaging network, *Magn. Reson. Imaging* 30 (9) (2012) 1323–1341, <https://doi.org/10.1016/j.mri.2012.05.001>.
- [18] S.D. Qanadli, M. El Hajjam, A. Vieillard-Baron, T. Joseph, B. Mesurolle, V.L. Oliva, O. Barré, F. Bruckert, O. Dubourg, P. Lacombe, New CT index to quantify arterial obstruction in pulmonary embolism: comparison with angiographic index and echocardiography, *Ajr. Am. J. Roentgenol.* 176 (6) (2001) 1415–1420, <https://doi.org/10.2214/ajr.176.6.1761415>.
- [19] D.C. Rotzinger, J.F. Knebel, A.M. Jouannic, G. Adler, S.D. Qanadli, CT pulmonary angiography for risk stratification of patients with nonmassive acute pulmonary embolism, *Radiol. Cardiothorac. Imaging* 2 (4) (2020), e190188, <https://doi.org/10.1148/ryct.2020190188>.
- [20] M.M. Mukaka, Statistics corner: a guide to appropriate use of correlation coefficient in medical research, *Malawi Med. J.: J. Med. Assoc. Malawi* 24 (3) (2012) 69–71.
- [21] N.R. Anthonisen, J. Milic-Emili, Distribution of pulmonary perfusion in erect man, *J. Appl. Physiol.* 21 (3) (1966) 760–766, <https://doi.org/10.1152/jappl.1966.21.3.760>.
- [22] W.C. Ball Jr., P.B. Stewart, L.G. Newsham, D.V. Bates, Regional pulmonary function studied with xenon 133, *J. Clin. Investig.* 41 (3) (1962) 519–531, <https://doi.org/10.1172/JCI104505>.
- [23] A.C. Bryan, L.G. Bentivoglio, F. Beerel, H. Macleish, A. Zidulka, D.V. Bates, Factors affecting regional distribution of ventilation and perfusion in the lung, *J. Appl. Physiol.* 19 (1964) 395–402, <https://doi.org/10.1152/jappl.1964.19.3.395>.
- [24] J.M. Hughes, J.B. Glazier, J.E. Maloney, J.B. West, Effect of lung volume on the distribution of pulmonary blood flow in man, *Respir. Physiol.* 4 (1) (1968) 58–72, [https://doi.org/10.1016/0034-5687\(68\)90007-8](https://doi.org/10.1016/0034-5687(68)90007-8).
- [25] K. Kaneko, J. Milic-Emili, M.B. Dolovich, A. Dawson, D.V. Bates, Regional distribution of ventilation and perfusion as a function of body position, *J. Appl. Physiol.* 21 (3) (1966) 767–777, <https://doi.org/10.1152/jappl.1966.21.3.767>.
- [26] J.B. West, Regional differences in the lung, *Chest* 74 (4) (1978) 426–437, <https://doi.org/10.1378/chest.74.4.426>.
- [27] Hopkins, S.R., Henderson, A.C., Levin, D.L., Yamada, K., Arai, T., Buxton, R.B., & Prisk, G.K. (2007). Vertical gradients in regional lung density and perfusion in the supine human lung: the Slinky effect. *Journal of applied physiology* (Bethesda, Md.: 1985), 103(1), 240–248. (<https://doi.org/10.1152/japplphysiol.01289.2006>).
- [28] M.N. Melsom, T. Flatebø, J. Kramer-Johansen, A. Aulie, O.V. Sjaastad, P.O. Iversen, G. Nicolaysen, Both gravity and non-gravity dependent factors determine regional blood flow within the goat lung, *Acta Physiol. Scand.* 153 (4) (1995) 343–353, <https://doi.org/10.1111/j.1748-1716.1995.tb09872.x>.
- [29] R.W. Glenny, L. Polissar, H.T. Robertson, Relative contribution of gravity to pulmonary perfusion heterogeneity, *J. Appl. Physiol.* (Bethesda, Md.: 1985) 71 (6) (1991) 2449–2452, <https://doi.org/10.1152/jappl.1991.71.6.2449>.
- [30] R.W. Glenny, W.J. Lamm, R.K. Albert, H.T. Robertson, Gravity is a minor determinant of pulmonary blood flow distribution, *J. Appl. Physiol.* (Bethesda, Md.: 1985) 71 (2) (1991) 620–629, <https://doi.org/10.1152/jappl.1991.71.2.620>.

- [31] R. Lisbona, G.W. Dean, T.S. Hakim, Observations with SPECT on the normal regional distribution of pulmonary blood flow in gravity independent planes, *J. Nucl. Med.: Off. Publ., Soc. Nucl. Med.* 28 (11) (1987) 1758–1762.
- [32] R.W. Glenny, Spatial correlation of regional pulmonary perfusion, *J. Appl. Physiol.* (1985) 72 (6) (1992) 2378–2386, <https://doi.org/10.1152/jappl.1992.72.6.2378>.
- [33] K.S. Burrowes, P.J. Hunter, M.H. Tawhai, Investigation of the relative effects of vascular branching structure and gravity on pulmonary arterial blood flow heterogeneity via an image-based computational model, *Acad. Radiol.* 12 (11) (2005) 1464–1474, <https://doi.org/10.1016/j.acra.2005.06.004>.
- [34] T.S. Hakim, R. Lisbona, G.W. Dean, Gravity-independent inequality in pulmonary blood flow in humans, *J. Appl. Physiol.* (Bethesda, Md.: 1985) 63 (3) (1987) 1114–1121, <https://doi.org/10.1152/jappl.1987.63.3.1114>.
- [35] W.A. Altemeier, H.T. Robertson, R.W. Glenny, Pulmonary gas-exchange analysis by using simultaneous deposition of aerosolized and injected microspheres, *J. Appl. Physiol.* (Bethesda, Md.: 1985) 85 (6) (1998) 2344–2351, <https://doi.org/10.1152/jappl.1998.85.6.2344>.
- [36] H. Koike, E. Sueyoshi, I. Sakamoto, M. Uetani, T. Nakata, K. Maemura, Quantification of lung perfusion blood volume (lung PBV) by dual-energy CT in patients with chronic thromboembolic pulmonary hypertension (CTEPH) before and after balloon pulmonary angioplasty (BPA): preliminary results, *Eur. J. Radiol.* 85 (9) (2016) 1607–1612, <https://doi.org/10.1016/j.ejrad.2016.06.016>.
- [37] K. Hsu, J.P. Williamson, M.J. Peters, A.J. Ing, Endoscopic lung volume reduction in COPD: improvements in gas transfer capacity are associated with improvements in ventilation and perfusion matching, *J. Bronchol. Interv. Pulmonol.* 25 (1) (2018) 48–53, <https://doi.org/10.1097/LBR.0000000000000445>.
- [38] E.J. Zucker, A. Kino, H. Schmiedeskamp, V. Hinojosa, D. Fleischmann, F.P. Chan, Feasibility and utility of dual-energy chest CTA for preoperative planning in pediatric pulmonary artery reconstruction, *Int. J. Cardiovasc. Imaging* 35 (8) (2019) 1473–1481, <https://doi.org/10.1007/s10554-019-01602-z>.